

Unusual spin Hall effect of a light beam in chiral metamaterials

Hailei Wang and Xiangdong Zhang*

Department of Physics, Applied Optics Beijing Area Major Laboratory, Beijing Normal University, Beijing 100875, China

(Received 27 January 2011; published 12 May 2011)

We present a solution to the problem of reflection and refraction of a polarized Gaussian beam at the interface between the transparent medium and the chiral metamaterials. Some unusual spin Hall effects of reflected and transmitted light have been found. It is shown that the spin-dependent displacements of the reflected beam centroid can not only reach several tens of wavelengths at certain incident angles; the reversed effect for the transmitted beams can also be realized by tuning the chiral parameters. These findings provide an alternative pathway for controlling the spin Hall effects of light and thereby open up the possibility for developing new nanophotonic devices.

DOI: [10.1103/PhysRevA.83.053820](https://doi.org/10.1103/PhysRevA.83.053820)

PACS number(s): 42.25.-p, 42.79.-e, 41.20.Jb, 78.20.Ci

I. INTRODUCTION

In the past few years there has been a great deal of interest in studying the spin Hall effect (SHE) owing to its potentialities in spintronics [1–3]. The SHE is driven by the spin state of the particles, which can be observed even in the absence of any scattering impurities when an electric field is applied to a semiconductor [1–3]. A photonic version of the effect was recently proposed [4,5] in which the spin photons play the role of the spin charges and a refractive index gradient plays the role of the electric potential gradient. Such a spatial gradient for the refractive index could occur at an interface between two materials. Thus, the SHE of light should be observed when a polarized light beam passes through the interface [4–8]. More recently, such an effect has been detected in experiments [9,10]. Furthermore, the SHE of light has also been found in other systems [11–18]. However, all these investigations focused on conventional media and the shift is generally less than one wavelength.

On the other hand, left-handed materials (LHMs) have attracted a great deal of attention from both theoretical and experimental sides [19–22]. These materials are characterized by simultaneous negative permittivity and permeability, which possess a number of unusual electromagnetic effects including negative refraction, inverse Snell's law, reversed Doppler shift, and reversed Cerenkov radiation [23]. These anomalous features allow considerable control over light propagation and open the door for new approaches to a variety of applications. However, recent studies show that the SHE of light in the LHMs is unreversed, although the sign of the refractive index gradient is reversed [24,25]. In fact, a negative index can be achieved alternatively through a chiral route [26–30]. The investigation of chiral metamaterials has also attracted much attention [26–31]. Although the reflection and refraction properties of the plane electromagnetic wave in the chiral negative refraction medium have been studied and the Goos-Hänchen shift has been analyzed [31–34], the SHE of light by the chiral metamaterials has not been discussed so far.

In this work, we provide an analytical solution for the reflection and refraction of a polarized Gaussian beam at the interface between the transparent medium and the chiral

metamaterials, with attention mainly focused on the SHE of light. We find that the SHE of light in the chiral metamaterials can not only reach several tens of wavelength for the reflected beam centroid at certain incident angles by tuning the chiral parameters; the reversed effect for the transmitted beam can also be realized. The rest of the paper is organized as follows. In Sec. III we present the theory and formula for the problem. The numerical results and discussions are described in Sec. III. A conclusion is given in Sec. IV.

II. THEORY AND FORMULA

We assume that an arbitrarily polarized beam propagating in a homogeneous isotropic dielectric medium is incident at an angle θ_i upon the surface of a chiral medium as shown in Fig. 1. The constitutive relations of the chiral medium are defined by [31]

$$\vec{D} = \varepsilon \vec{E} + i \frac{\kappa}{c} \vec{H}, \quad (1)$$

$$\vec{B} = \mu \vec{H} - i \frac{\kappa}{c} \vec{E}, \quad (2)$$

where κ is the chirality parameter and c is the optical velocity in vacuum; ε and μ are the relative permittivity and permeability of the chiral medium, respectively. Inside the chiral medium the beam splits into two transmitted waves: a right-handed circularly polarized (RCP) wave with phase velocity ω/k_1 and a left-handed circularly polarized (LCP) wave with phase velocity ω/k_2 , where the wave numbers are given by $k_{1,2} = k_0 n_{1,2} = k_0(\sqrt{\varepsilon\mu} \pm \kappa)$. Here $n_1 = \sqrt{\varepsilon\mu} + \kappa$ ($n_2 = \sqrt{\varepsilon\mu} - \kappa$) is defined as the index of the RCP(LCP) waves; $k_0 = \omega/c$ denotes the wave number in the vacuum. The z axis of the laboratory Cartesian frame (x, y, z) is normal to the interface of the chiral medium located at $z = 0$. We use the coordinate frames $(x_\alpha, y_\alpha, z_\alpha)$ for individual beams, where $\alpha = i, r, 1, 2$ denotes incident, reflected, and two transmitted beams, respectively. In paraxial optics, the incident field of an arbitrarily polarized beam can be written as [5,7,24],

$$\vec{E}_i(x_i, y_i, z_i) = (E_{ix}\hat{e}_{ix} + E_{iy}\hat{e}_{iy}) \exp\left[-\frac{k_0}{2} \frac{x_i^2 + y_i^2}{Z_R + iz_r}\right]. \quad (3)$$

*Corresponding author; zhangxd@bnu.edu.cn

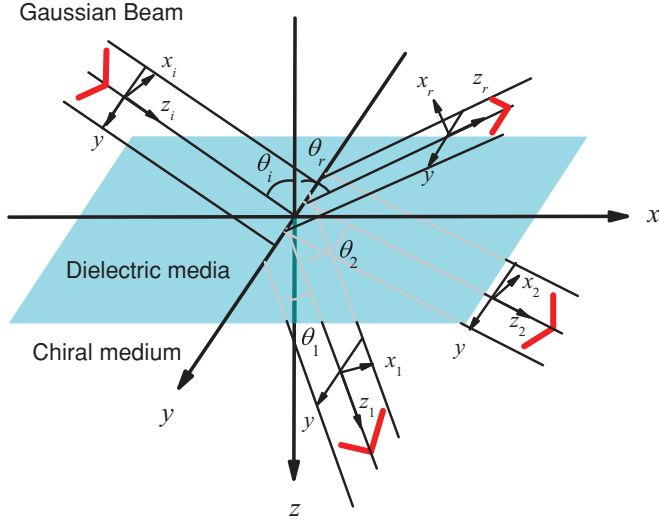


FIG. 1. (Color online) Geometry of the beam reflection and transmission from an air-chiral medium interface. The subscripts i and r represent the incident and reflection beams, respectively, whereas 1 and 2 correspond to transmitted RCP and LCP waves.

Here $Z_R = k_0 w_0^2/2$ is the Rayleigh length; w_0 is the minimum waist which characterizes the Gaussian amplitude. The complex-valued vectors E_{ix} and E_{iy} determine the polarization of the incident beam, which satisfies the relation $\sigma = i(E_{ix}E_{iy}^* - E_{ix}^*E_{iy})$. The polarization operator $\sigma = \pm 1$ corresponds to the LCP and the RCP lights, respectively. The reflected field can be solved by employing Fourier transformations. The complex amplitude can be conveniently expressed as

$$\vec{E}_r(x_r, y_r, z_r) = \int dk_{rx} dk_{ry} \vec{E}_r(k_{rx}, k_{ry}) \times \exp[i(k_{rx}x_r + k_{ry}y_r + k_{rz}z_r)], \quad (4)$$

where $k_{rx} = -k_{ix}$ and $k_{rz} = k_{iz}$ are the components of the wave vector (k_r) of the reflection beam. By using the boundary conditions at the interface in the paraxial approximation [$k_{rz} \simeq k_r - (k_{rx}^2 + k_{ry}^2)/2k_r$], the reflected angular spectrum $\vec{E}_r(k_{rx}, k_{ry})$ which is related to the boundary distribution of the electric field can be expressed as

$$\vec{E}_r(k_{rx}, k_{ry}) = \begin{pmatrix} r_{11} + \frac{k_{ry}}{k_0} (r_{21} - r_{12}) \cot \theta_i & r_{12} + \frac{k_{ry}}{k_0} (r_{11} + r_{22}) \cot \theta_i \\ r_{21} - \frac{k_{ry}}{k_0} (r_{11} + r_{22}) \cot \theta_i & r_{22} + \frac{k_{ry}}{k_0} (r_{21} - r_{12}) \cot \theta_i \end{pmatrix} \begin{pmatrix} E_{ix} \\ E_{iy} \end{pmatrix} \exp \left[-\frac{Z_R(k_{rx}^2 + k_{ry}^2)}{2k_0} \right]. \quad (5)$$

Here r_{11} , r_{12} , r_{21} , and r_{22} are the reflection coefficients which are given in Appendix A. Inserting Eq. (5) into Eq. (4), the reflected field at $z_r > 0$ can be expressed as

$$\begin{aligned} \vec{E}_r(x_r, y_r) = & \left[r_{11} \left(1 - i \frac{x_r}{Z_R + iz_r} \frac{\partial}{\partial \theta_i} \ln r_{11} \right) E_{ix} + r_{12} \left(1 - i \frac{x_r}{Z_R + iz_r} \frac{\partial}{\partial \theta_i} \ln r_{12} \right) E_{iy} + i \frac{y_r}{Z_R + iz_r} (r_{21} - r_{12}) E_{ix} \cot \theta_i \right. \\ & \left. + i \frac{y_r}{Z_R + iz_r} (r_{11} + r_{22}) E_{iy} \cot \theta_i \right] \exp \left[-\frac{k_0(x_r^2 + y_r^2)}{2(Z_R + iz_r)} \right] \hat{e}_{rx} + \left[r_{21} \left(1 - i \frac{x_r}{Z_R + iz_r} \frac{\partial}{\partial \theta_i} \ln r_{21} \right) E_{ix} \right. \\ & \left. + r_{22} \left(1 - i \frac{x_r}{Z_R + iz_r} \frac{\partial}{\partial \theta_i} \ln r_{22} \right) E_{iy} - i \frac{y_r}{Z_R + iz_r} (r_{11} + r_{22}) E_{ix} \cot \theta_i + i \frac{y_r}{Z_R + iz_r} (r_{21} - r_{12}) E_{iy} \cot \theta_i \right] \\ & \times \exp \left[-\frac{k_0(x_r^2 + y_r^2)}{2(Z_R + iz_r)} \right] \hat{e}_{ry}. \end{aligned} \quad (6)$$

Similarly, the transmitted field is expressed as

$$\vec{E}_a(x_a, y_a, z_a) = \int dk_{ax} dk_{ay} \vec{E}_a(k_{ax}, k_{ay}) \exp[i(k_{ax}x_a + k_{ay}y_a + k_{az}z_a)], \quad (7)$$

where $a = 1, 2$ represents the RCP and the LCP transmitted fields, respectively. With $k_{az} \simeq k_a - (k_{ax}^2 + k_{ay}^2)/2k_a$ and the boundary distribution of the electric field, the transmitted angular spectrum can be expressed as

$$\vec{E}_a(k_{ax}, k_{ay}) = \begin{pmatrix} t_{11}^a - \frac{k_{ay}}{k_0} (t_{12}^a + \eta_a t_{21}^a) \cot \theta_i & t_{12}^a + \frac{k_{ay}}{k_0} (t_{11}^a - \eta_a t_{22}^a) \cot \theta_i \\ t_{21}^a + \frac{k_{ay}}{k_0} (\eta_a t_{11}^a - t_{22}^a) \cot \theta_i & t_{22}^a + \frac{k_{ay}}{k_0} (\eta_a t_{12}^a + t_{21}^a) \cot \theta_i \end{pmatrix} \begin{pmatrix} E_{ix} \\ E_{iy} \end{pmatrix} \exp \left[-\frac{Z_{ax}k_{ax}^2 + Z_{ay}k_{ay}^2}{2n_a k_0} \right], \quad (8)$$

where t_{11}^a , t_{12}^a , t_{21}^a , and t_{22}^a are the corresponding transmission coefficients of the RCP and LCP waves which are given in Appendix A. Here $\eta_a = \cos \theta_a / \cos \theta_i$; θ_a is the refraction angle. From Snell's law under the paraxial approximation, $k_{ax} = k_{ix} / \eta_a$ and $k_{ay} = k_{iy}$, and $Z_{ax} = n_a \eta_a^2 k_0 w_0^2 / 2$ and $Z_{ay} = n_a k_0 w_0^2 / 2$. Substituting Eq. (8) into Eq. (7), we obtain the transmitted field in

the space $z_a > 0$,

$$\begin{aligned} \vec{E}_a(x_a, y_a) = & \left[t_{11}^a \left(1 + i \frac{n_a \eta_a x_a}{Z_{ax} + i z_a} \frac{\partial}{\partial \theta_i} \ln t_{11}^a \right) E_{ix} + t_{12}^a \left(1 + i \frac{n_a \eta_a x_a}{Z_{ax} + i z_a} \frac{\partial}{\partial \theta_i} \ln t_{12}^a \right) E_{iy} - i \frac{n_a y_a}{Z_{ay} + i z_a} (t_{12}^a + \eta_a t_{21}^a) \right. \\ & \times E_{ix} \cot \theta_i + i \frac{n_a y_a}{Z_{ay} + i z_a} (t_{11}^a - \eta_a t_{22}^a) E_{iy} \cot \theta_i \left. \right] \exp \left[-\frac{n_a k_0}{2} \left(\frac{x_a^2}{Z_{ax} + i z_a} + \frac{y_a^2}{Z_{ay} + i z_a} \right) \right] \hat{e}_{ax} \\ & + \left[t_{21}^a \left(1 + i \frac{n_a \eta_a x_a}{Z_{ax} + i z_a} \frac{\partial}{\partial \theta_i} \ln t_{21}^a \right) E_{ix} + t_{22}^a \left(1 + i \frac{n_a \eta_a x_a}{Z_{ax} + i z_a} \frac{\partial}{\partial \theta_i} \ln t_{22}^a \right) E_{iy} + i \frac{n_a y_a}{Z_{ay} + i z_a} (\eta_a t_{11}^a - t_{22}^a) E_{ix} \cot \theta_i \right. \\ & \left. + i \frac{n_a y_a}{Z_{ay} + i z_a} (t_{21}^a + \eta_a t_{12}^a) E_{iy} \cot \theta_i \right] \exp \left[-\frac{n_a k_0}{2} \left(\frac{x_a^2}{Z_{ax} + i z_a} + \frac{y_a^2}{Z_{ay} + i z_a} \right) \right] \hat{e}_{ay}. \end{aligned} \quad (9)$$

After the electric fields of the reflected and two transmitted beams are obtained, the time-averaged linear momentum density associated with the electromagnetic field can be shown to be $\vec{p}_\alpha \propto \text{Re}(\vec{E}_\alpha^* \times \vec{H}_\alpha)$. \vec{H}_α represents the magnetic field in the dielectric and chiral media, which is given by $\vec{H}_r = -i(\mu\omega)^{-1} \nabla \times \vec{E}_r$ and $\vec{H}_a = -i(\mu\omega)^{-1} (\nabla \times \vec{E}_a - \kappa k_0 \vec{E}_a)$. Then, the intensity distribution of the electromagnetic field, $I \propto \vec{p}_\alpha \cdot \hat{e}_{\alpha z}$, can be obtained. At any given plane $z_\alpha = \text{const}$, the beam centroid is expressed as

$$\langle x_\alpha \rangle = \frac{\int \int x_\alpha I(x_\alpha, y_\alpha, z_\alpha) dx_\alpha dy_\alpha}{\int \int I(x_\alpha, y_\alpha, z_\alpha) dx_\alpha dy_\alpha} \quad (10)$$

$$\langle y_\alpha \rangle = \frac{\int \int y_\alpha I(x_\alpha, y_\alpha, z_\alpha) dx_\alpha dy_\alpha}{\int \int I(x_\alpha, y_\alpha, z_\alpha) dx_\alpha dy_\alpha}.$$

Substituting Eq. (6) into Eq. (10), we can obtain the longitudinal and the transverse shifts of the centroid of the reflected beam in the following:

$$D_{rx} = \frac{\Delta_{rx}}{k_0 \tau} + \frac{z_r}{Z_R} \frac{\delta_{rx}}{k_0 \tau}, \quad (11)$$

$$D_{ry} = \frac{\Delta_{ry}}{k_0 \tau} + \frac{z_r}{Z_R} \frac{\delta_{ry}}{k_0 \tau}. \quad (12)$$

Both Eqs. (11) and (12) can be written as a combination of z_r -dependent terms ($\Delta_{rx}/k_0 \tau$ or $\Delta_{ry}/k_0 \tau$) and z_r -independent terms [$z_r \delta_{rx}/(Z_R k_0 \tau)$ or $z_r \delta_{ry}/(Z_R k_0 \tau)$]. For a well-collimated beam, the condition $z_r/Z_R \ll 1$ is trivially satisfied and the z_r -independent terms are dominant, while for a focused beam the condition $z_r/Z_R \gg 1$ may hold and the z_r -independent terms become relevant. The analytical expressions for Δ_{rx} , δ_{rx} , Δ_{ry} , δ_{ry} , and τ are given in Appendix B. These expressions include the coefficients f_p and f_s , which satisfy the relations $E_{ix} = f_p \in \mathbf{R}$ and $E_{iy} = f_s \exp(i\psi)$, respectively. Here ψ denotes the phase difference for two polarized fields. Similarly, the corresponding shifts for the RCP and LCP transmitted beams are given as

$$D_{ax} = \frac{\eta_a \Delta_{ax}}{k_0 \tau_a} + \frac{z_a}{Z_{Rx}} \frac{\eta_a \delta_{ax}}{k_0 \tau_a}, \quad (13)$$

$$D_{ay} = \frac{\eta_a \Delta_{ay}}{k_0 \tau_a} + \frac{z_a}{Z_{Ry}} \frac{\eta_a \delta_{ay}}{k_0 \tau_a}. \quad (14)$$

The longitudinal and transverse shifts for the transmitted beams can also be separated into two terms: a z_a -dependent term and z_a -independent term. The analytical expressions for Δ_{ax} , δ_{ax} , Δ_{ay} , δ_{ay} , and τ_a are also given in Appendix B. Based on Eqs. (11)–(14), the longitudinal and the transverse shifts of the reflected and transmitted beams can be obtained exactly.

III. NUMERICAL RESULTS AND DISCUSSION

We first consider the SHE of the reflected beam at an air-chiral medium interface for a circularly polarized incident Gaussian beam. The calculated results for the transverse spatial shifts of the reflected beam (D_{ry}/λ) as a function of the incident angle are plotted in Fig. 2. Figures 2(a)–2(d), corresponding to the cases with $\kappa = 0, 0.5, 1.0$, and 1.4 , respectively. The other parameters are taken as $\varepsilon = 2.0$, $\mu = 1$, $\psi = -\pi/2$, and $f_s = f_p = 1$. As $\kappa = 0$, our results are agreement with the previous investigations [5, 9, 24], the shift is generally less than one wavelength. However, with the increase of κ , the SHE can be greatly tuned. At certain incident angles, large SHE can be found. For example, D_{ry}/λ is 0.67 at $\kappa = 1.0$ and $\theta_i = 24.5^\circ$, while it reaches 21.4 at $\kappa = 1.4$ and $\theta_i = 0.8^\circ$. The physical origin of these phenomena can be understood with the angular-momentum conservation law. The z component of the total angular momentum per one photon can be represented as the sum of the extrinsic orbital angular momentum and intrinsic spin angular momentum:

$$j_{rz} = -\Delta_{ry} k_r \sin \theta_r + \sigma_r \cos \theta_r, \quad (15)$$

$$j_{1z} = -\Delta_{1y} k_1 \sin \theta_1 + \sigma_1 \cos \theta_1, \quad (16)$$

$$j_{2z} = -\Delta_{2y} k_2 \sin \theta_2 + \sigma_2 \cos \theta_2, \quad (17)$$

where σ_r, σ_1 , and σ_2 are the polarization degrees of the reflected and two transmitted beams, which are described by

$$\sigma_r = \frac{2f_p f_s [|r_{21}| |r_{12}| \sin(\phi_{21} - \phi_{12} - \psi) + |r_{11}| |r_{22}| \sin(\phi_{22} - \phi_{11} + \psi)]}{f_s^2 (|r_{22}|^2 + |r_{12}|^2) + f_p^2 (|r_{11}|^2 + |r_{21}|^2)}, \quad (18)$$

$$\sigma_1 = -1 \text{ and } \sigma_2 = 1. \quad (19)$$

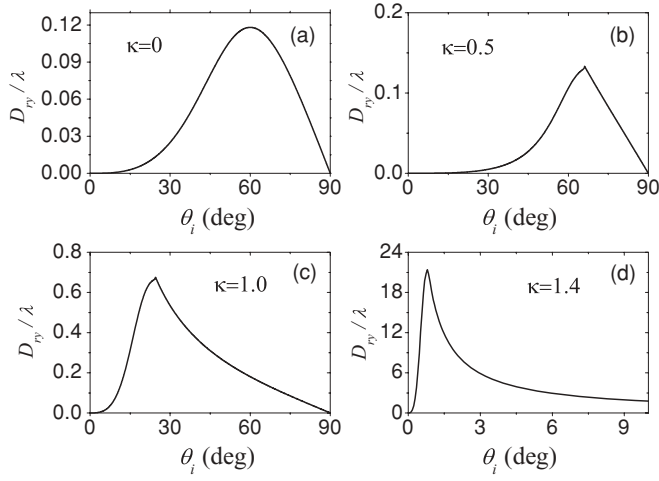


FIG. 2. Normalized transverse spatial shifts of the reflection beam (D_{ry}/λ) as a function of the incident angle for a circularly polarized incident Gaussian beam. (a), (b), (c), and (d) correspond to the cases with $\kappa = 0, 0.5, 1.0$, and 1.4 , respectively. The other parameters are taken as $\varepsilon = 2.0$, $\mu = 1$, $\psi = -\pi/2$, and $f_s = f_p = 1$.

The transverse shifts of the wave packet fulfill the conservation law for the total angular momentum:

$$Q_r j_{rz} + Q_1 j_{1z} + Q_2 j_{2z} = j_{iz}. \quad (20)$$

Here $Q_r = f_s^2(|r_{22}|^2 + |r_{12}|^2) + f_p^2(|r_{11}|^2 + |r_{21}|^2)$, $Q_1 = n_1 \eta_1 [f_p^2(|t_{11}^1|^2 + |t_{21}^1|^2) + f_s^2(|t_{12}^1|^2 + |t_{22}^1|^2)]$, and $Q_2 = n_2 \eta_2 [f_p^2(|t_{11}^2|^2 + |t_{21}^2|^2) + f_s^2(|t_{12}^2|^2 + |t_{22}^2|^2)]$ are the energy reflection and transmission coefficients for the RCP and the LCP waves, respectively; $j_{iz} = \sigma \cos \theta_i$. As $\kappa = 0$, Eq. (20) reduces to the form in Refs. [5,24]:

$$Q_r j_{rz} + Q_t j_{tz} = j_{iz}, \quad (21)$$

with $j_{rz} = j_{rz}^o + j_{rz}^s$ and $j_{tz} = j_{tz}^o + j_{tz}^s$. In such a case, the transmitted beam is not split into the RCP and the LCP waves. Thus, the subscripts 1 and 2 in Eq. (20) are replaced by t . Here $j_{rz}^o = -\Delta_{ry} k_r \sin \theta_r$ and $j_{tz}^o = -\Delta_{ty} k_t \sin \theta_t$ are the orbital angular momentums for the reflected and transmitted beams, respectively; $j_{rz}^s = \sigma_r \cos \theta_r$ and $j_{tz}^s = \sigma_t \cos \theta_t$ are the corresponding spin angular momentums. The analytical expressions for σ_r , σ_t , Q_r , and Q_t in Eq. (21) are given in Ref. [24].

In order to reveal the physics underlying the maximums of transverse spatial shifts at certain incident angles, we plot total angular momentums as a function of the incident angle in Fig. 3. Here $\kappa = 0$ is taken, which corresponds to the case in Fig. 2(a). The solid line, dashed line, and dotted line represent the total angular momentums for incident, reflected, and transmitted beams, respectively. As can be seen, they satisfy the conservation law for the total angular momentum very well. At $\theta_i = 45^\circ$, a sharp transition appears for the total angular momentums of reflected and transmitted beams due to the total reflection. As $\theta_i > 45^\circ$, the total angular momentum of the transmitted beam vanishes. To ensure the conservation of total angular momentum, the total angular momentum of

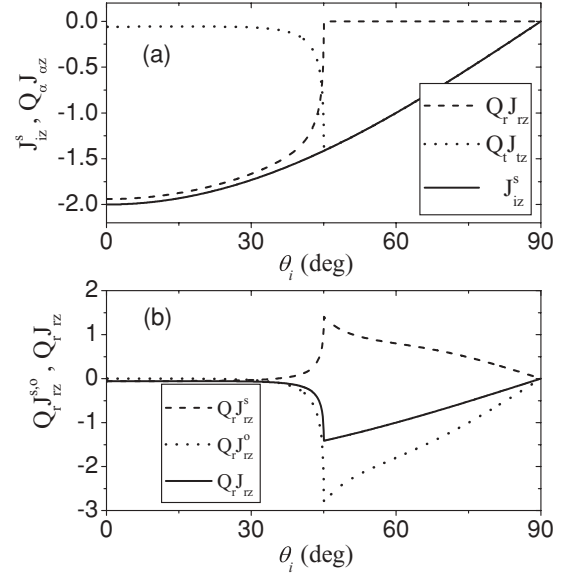


FIG. 3. The angular momentums as a function of the incident angle. (a) The total angular momentums for incident, reflected, and transmitted beams. (b) The spin angular momentum, orbital angular momentum, and total angular momentum for the reflected beam. The parameters are taken identical to those in Fig 2(a).

the reflected beam is equal to the incident one. It consists of the spin angular momentum and the orbital angular momentum. At the critical angle ($\theta_i = 45^\circ$) of the total reflection, the spin angular momentum of the reflected beam reaches the positive maximum, which leads to the negative maximum of the orbital angular momentum (or the transverse spatial shift). Such a phenomenon is shown clearly in Fig. 3(b). For the cases of $\kappa \neq 0$ [Figs. 2(b), 2(c), and 2(d)], the phenomena can be understood in the same way. That is to say, tuning the chirality parameter can cause the change of the total and the spin angular momentums, which results in the large transverse spatial shift of the reflected beam.

Figure 4 shows normalized transverse spatial shifts of the reflection beams (D_{ry}/λ) as a function of the chirality parameter κ for the circularly polarized incident Gaussian beam. The solid line, dashed line, and dotted line correspond to the cases with the incident angle $\theta_i = \pi/12$, $\pi/6$, and $\pi/3$ respectively. Recent investigations show that an important feature of the chiral metamaterials is that the negative index can be realized by tuning the chiral parameters. For example, as $\kappa > 1.414$, it is the negative refraction region for the present chiral medium, whereas $\kappa < 1.414$ corresponds to the positive refraction region. From Fig. 4, we see that the SHE in the two regions is symmetrical; the transverse shifts caused by the SHE in the negative refraction region are unreversed, although the sign of the refractive index gradient is reversed. Such a phenomenon is similar to the case in the conventional LHMs, which has been analyzed in Refs. [24,25].

In general, there is no transverse spatial shift when the polarized Gaussian beam with $f_s = 0$ or $f_p = 0$ is incident on the interface between two transparent media. However, for the chiral metamaterials, it is not real. Figure 5(a) displays normalized transverse spatial shifts of the reflection beam (D_{ry}/λ) as a function of the incident angle for the polarized

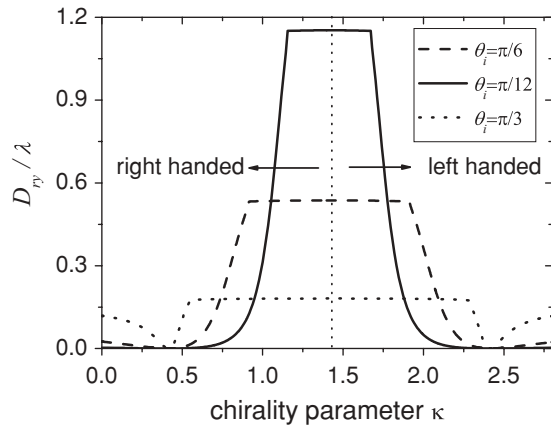


FIG. 4. Normalized transverse spatial shifts of the reflection beam (D_{ry}/λ) as a function of the chirality parameter for a circularly polarized incident Gaussian beam. The other parameters are taken as $\varepsilon = 2$, $\mu = 1$, $\psi = -\pi/2$, and $f_s = f_p = 1$. Solid, dashed, and dotted lines correspond to the incident angle $\theta_i = \pi/12$, $\pi/6$, and $\pi/3$ respectively.

incident Gaussian beam with $f_s = 0$. The solid line, dashed line, and dotted line correspond to the cases with $\kappa = 0.01$, 0.05 , and 0.1 , respectively. It is seen clearly that the resonant transverse spatial shift appears around the incident angle $\theta_i = 54.8^\circ$. This corresponds to the resonant transmission at

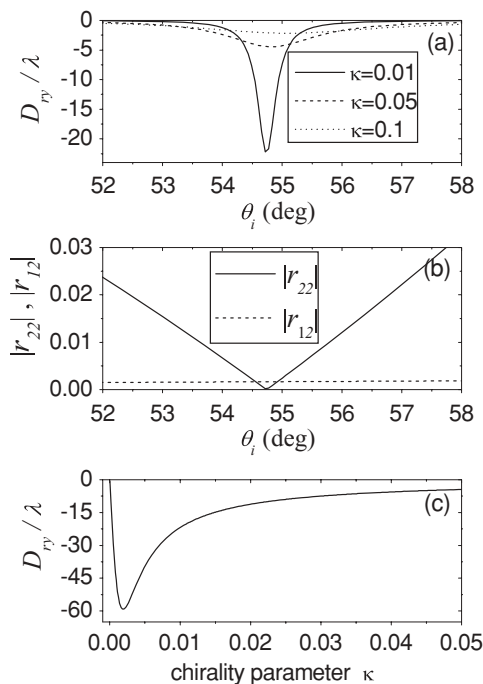


FIG. 5. (a) Normalized transverse spatial shifts of the reflection beam (D_{ry}/λ) as a function of the incident angle for a linearly polarized incident Gaussian beam. Solid, dashed, and dotted lines correspond to the cases with $\kappa = 0.01$, 0.05 , and 0.1 , respectively. (b) The corresponding reflection matrix elements $|r_{22}|$ (solid line) and $|r_{12}|$ (dashed line). (c) Normalized transverse spatial shifts of the reflection beam (D_{ry}/λ) as a function of the chirality parameter for a linearly polarized incident Gaussian beam at $\theta_i = 54.8^\circ$. The other parameters are taken as $\varepsilon = 2$, $\mu = 1$, $f_p = 1$, and $f_s = 0$.

the interface of the chiral medium. Figure 5(b) shows the reflection matrix elements $|r_{22}|$ (solid line) and $|r_{12}|$ (dashed line) as a function of the incident angle. Comparing Fig. 5(a) with Fig. 5(b), we find that the maximum of the transverse spatial shift of the reflected beam corresponds to the minimum of the reflection matrix elements $|r_{22}|$. Such a phenomenon can also be tuned by the chiral parameter as shown in Fig. 5(c), which results in the appearance of large SHE at certain incident angles. For example, the transverse spatial shift can reach 59.2λ at $\theta_i = 54.8^\circ$ and $\kappa = 0.01$.

The above discussions focused on the SHE of the reflected beam. We now turn to the case of the transmitted beam. The previous investigations have shown that the LCP beam undergoes a negative (positive) transverse shift, while the RCP beam exhibits a positive (negative) transverse shift in the case of the beam incident from air to the conventional medium [9,24]. The shifts for two kinds of polarized beams are symmetrical. However, with the introduction of the chiral parameters, the situation becomes different. Figures 6(a)–6(d) show transverse spatial shifts of the transmitted beam (D_{ty}/λ) as a function of the incident angle for the cases with $\kappa = 0$, 0.2 , 0.4 , and 0.6 , respectively. The solid line and dashed line correspond to the RCP and the LCP transmitted waves, respectively. As can be seen, with the increase of κ , the shifts for two kinds of polarized beams become asymmetrical. As $\kappa = 0.414$, the transition from negative shift to positive shift for the LCP transmitted waves occurs.

Such a transition is not related to the negative index. Figure 7(a) shows transverse spatial shifts of the RCP (solid line) and the LCP (dashed line) transmitted beams (D_{ty}/λ) as a function of the chirality parameter for the elliptical polarized incident Gaussian beam. The symmetric properties in two regions are observed again. At the same time, the resonant phenomenon of the transverse spatial shift for the RCP transmitted beam (the total reflection appears for the LCP

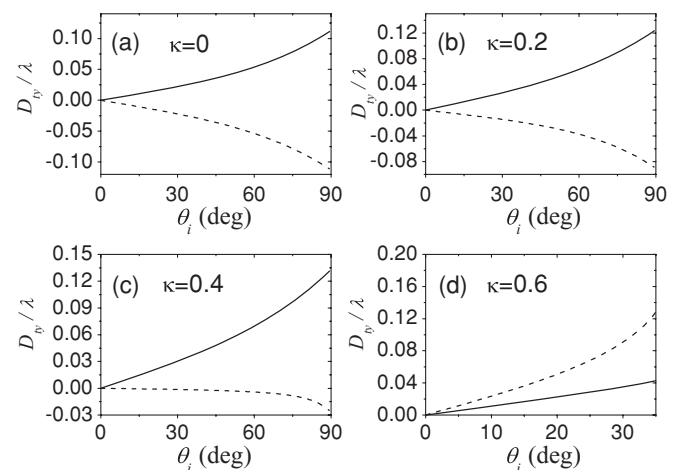


FIG. 6. Normalized transverse spatial shifts of the transmission beam (D_{ty}/λ) as a function of the incident angle for an elliptical polarized incident Gaussian beam. (a), (b), (c), and (d) correspond to the cases with $\kappa = 0$, 0.2 , 0.4 , and 0.6 , respectively. Solid line and dashed line correspond to the RCP and the LCP transmission waves, respectively. The other parameters are taken as $\varepsilon = 2$, $\mu = 1$, $\psi = 0$, and $f_s = f_p = 1$.

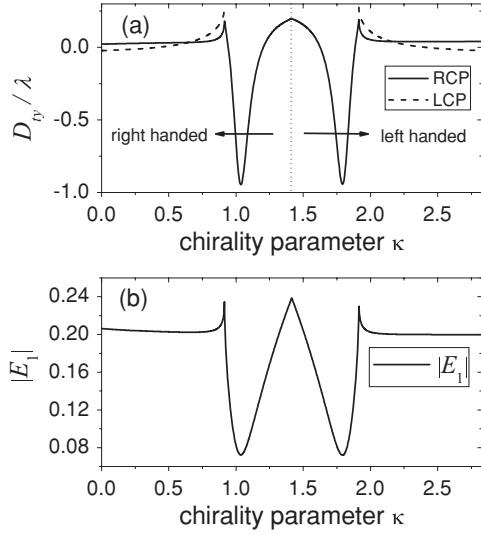


FIG. 7. (a) Normalized transverse spatial shifts of the transmission beam (D_{ty}/λ) as a function of the chirality parameter for a linearly polarized incident Gaussian beam. Solid line and dashed line correspond to the RCP and the LCP transmission waves, respectively. (b) The corresponding amplitude of the transmission electric field with RCP light. The other parameters are taken as $\varepsilon = 2$, $\mu = 1$, $\psi = -\pi/3$, $\theta_i = \pi/6$, and $f_s = f_p = 1$.

transmitted beam in some regions) has also been observed. At the resonant points, the transverse spatial shifts by the SHE reach maximum, which correspond to the resonant peaks of the transmission electric field of the RCP light as shown in Fig. 7(b). This means that the resonant transmission of the wave at the interface not only causes large SHE for the reflected beam; it also leads to large SHE for the transmitted beam. The physical origin is similar for both cases, which can be understood very well given the angular-momentum conservation law.

IV. CONCLUSION

In summary, we have presented an analytical solution to the problem of reflection and refraction of the polarized Gaussian

beam at the interface between the transparent medium and the chiral metamaterials. We have paid special attention to the transverse shifts of the centers of the reflected and refracted beams. It has been shown that the spin-dependent displacements of the reflected beam centroid can reach several tens of wavelengths at certain incident angles for both circularly and linearly polarized incident Gaussian beams. The reversed effect for the transmitted beam can also be observed by tuning the chiral parameters. With the development of recent technology, the chiral metamaterials can be fabricated successfully [30,31,33]. Thus, our findings provide an alternative pathway for controlling the SHE of light and open up the possibility for developing new nanophotonic devices.

ACKNOWLEDGMENTS

This work was supported by the National Natural Science Foundation of China (Grant No. 10825416) and the National Key Basic Research Special Foundation of China under Grant No. 2007CB613205 and Scientific Research Foundation of Beijing Normal University.

APPENDIX A

In this appendix we give the concrete expressions of the reflection and transmission coefficients at the interface between the transparent medium and the chiral metamaterials. If we define E_{ix} and E_{iy} as the amplitudes of the incident TM and TE waves, E_{rx} and E_{ry} as the corresponding values of the reflection wave, and E_1 and E_2 as the amplitudes of the transmitted RCP and LCP waves, the relations among them can be obtained by using the Maxwell equation and the boundary conditions:

$$\begin{pmatrix} E_{rx} \\ E_{ry} \end{pmatrix} = \begin{pmatrix} r_{11} & r_{12} \\ r_{21} & r_{22} \end{pmatrix} \begin{pmatrix} E_{ix} \\ E_{iy} \end{pmatrix} \quad (\text{A1})$$

and

$$\begin{pmatrix} E_1 \\ E_2 \end{pmatrix} = \begin{pmatrix} t_{11}^1 & t_{12}^1 \\ t_{11}^2 & t_{12}^2 \end{pmatrix} \begin{pmatrix} E_{ix} \\ E_{iy} \end{pmatrix}, \quad (\text{A2})$$

where the reflection and transmission coefficients r_{11} , r_{12} , r_{21} , r_{22} , t_{11}^a , t_{12}^a , t_{21}^a , and t_{22}^a are expressed as

$$r_{11} = -\frac{\cos \theta_i (1 - g^2)(\cos \theta_1 + \cos \theta_2) - 2g(\cos^2 \theta_i - \cos \theta_1 \cos \theta_2)}{\cos \theta_i (1 + g^2)(\cos \theta_1 + \cos \theta_2) + 2g(\cos^2 \theta_i + \cos \theta_1 \cos \theta_2)}, \quad (\text{A3})$$

$$r_{12} = \frac{2ig \cos \theta_i (\cos \theta_1 - \cos \theta_2)}{\cos \theta_i (1 + g^2)(\cos \theta_1 + \cos \theta_2) + 2g(\cos^2 \theta_i + \cos \theta_1 \cos \theta_2)}, \quad (\text{A4})$$

$$r_{21} = \frac{-2ig \cos \theta_i (\cos \theta_1 - \cos \theta_2)}{\cos \theta_i (1 + g^2)(\cos \theta_1 + \cos \theta_2) + 2g(\cos^2 \theta_i + \cos \theta_1 \cos \theta_2)}, \quad (\text{A5})$$

$$r_{22} = \frac{\cos \theta_i (1 - g^2)(\cos \theta_1 + \cos \theta_2) + 2g(\cos^2 \theta_i - \cos \theta_1 \cos \theta_2)}{\cos \theta_i (1 + g^2)(\cos \theta_1 + \cos \theta_2) + 2g(\cos^2 \theta_i + \cos \theta_1 \cos \theta_2)}, \quad (\text{A6})$$

$$t_{11}^1 = \frac{2 \cos \theta_i (\cos \theta_i + g \cos \theta_2)}{\cos \theta_i (1 + g^2)(\cos \theta_1 + \cos \theta_2) + 2g(\cos^2 \theta_i + \cos \theta_1 \cos \theta_2)}, \quad (\text{A7})$$

$$t_{12}^1 = \frac{-2i \cos \theta_i (g \cos \theta_i + \cos \theta_2)}{\cos \theta_i (1 + g^2)(\cos \theta_1 + \cos \theta_2) + 2g(\cos^2 \theta_i + \cos \theta_1 \cos \theta_2)}, \quad (\text{A8})$$

$$t_{21}^1 = \chi_1 \frac{2 \cos \theta_i (\cos \theta_i + g \cos \theta_2)}{\cos \theta_i (1 + g^2)(\cos \theta_1 + \cos \theta_2) + 2g(\cos^2 \theta_i + \cos \theta_1 \cos \theta_2)}, \quad (\text{A9})$$

$$t_{22}^1 = \chi_1 \frac{-2i \cos \theta_i (g \cos \theta_i + \cos \theta_2)}{\cos \theta_i (1 + g^2) (\cos \theta_1 + \cos \theta_2) + 2g (\cos^2 \theta_i + \cos \theta_1 \cos \theta_2)}, \quad (\text{A10})$$

$$t_{11}^2 = \frac{2 \cos \theta_i (\cos \theta_i + g \cos \theta_1)}{\cos \theta_i (1 + g^2) (\cos \theta_1 + \cos \theta_2) + 2g (\cos^2 \theta_i + \cos \theta_1 \cos \theta_2)}, \quad (\text{A11})$$

$$t_{12}^2 = \frac{2i \cos \theta_i (g \cos \theta_i + \cos \theta_1)}{\cos \theta_i (1 + g^2) (\cos \theta_1 + \cos \theta_2) + 2g (\cos^2 \theta_i + \cos \theta_1 \cos \theta_2)}, \quad (\text{A12})$$

$$t_{21}^2 = \chi_2 \frac{2 \cos \theta_i (\cos \theta_i + g \cos \theta_1)}{\cos \theta_i (1 + g^2) (\cos \theta_1 + \cos \theta_2) + 2g (\cos^2 \theta_i + \cos \theta_1 \cos \theta_2)}, \quad (\text{A13})$$

$$t_{22}^2 = \chi_2 \frac{2i \cos \theta_i (g \cos \theta_i + \cos \theta_1)}{\cos \theta_i (1 + g^2) (\cos \theta_1 + \cos \theta_2) + 2g (\cos^2 \theta_i + \cos \theta_1 \cos \theta_2)}. \quad (\text{A14})$$

Here $g = \sqrt{\frac{\epsilon}{\mu}}$, $\chi_{12} = \pm i$, and θ_{12} correspond to the refraction angle of the RCP and the LCP waves in the chiral medium.

APPENDIX B

In this appendix we give the concrete expressions for Δ_{rx} , δ_{rx} , Δ_{ry} , δ_{ry} , τ , Δ_{ax} , δ_{ax} , Δ_{ay} , δ_{ay} , and τ_a in Eqs. (11)–(14):

$$\begin{aligned} \Delta_{rx} = & f_s^2 (|r_{22}|^2 \xi_{22} + |r_{12}|^2 \xi_{12}) + f_p^2 (|r_{11}|^2 \xi_{11} + |r_{21}|^2 \xi_{21}) \\ & + f_p f_s [|r_{22}| |r_{21}| (\xi_{22} + \xi_{21}) \cos(\phi_{22} - \phi_{21} + \psi) \\ & + |r_{11}| |r_{12}| (\xi_{11} + \xi_{12}) \cos(\phi_{12} - \phi_{11} + \psi) \\ & + |r_{11}| |r_{12}| (\rho_{12} - \rho_{11}) \sin(\phi_{12} - \phi_{11} + \psi) \\ & + |r_{22}| |r_{21}| (\rho_{21} - \rho_{22}) \sin(\phi_{21} - \phi_{22} - \psi)], \quad (\text{B1}) \end{aligned}$$

$$\begin{aligned} \delta_{rx} = & -f_s^2 (|r_{22}|^2 \rho_{22} + |r_{12}|^2 \rho_{12}) - f_p^2 (|r_{11}|^2 \rho_{11} + |r_{21}|^2 \rho_{21}) \\ & + f_p f_s [-|r_{22}| |r_{21}| (\rho_{22} + \rho_{21}) \cos(\phi_{22} - \phi_{21} + \psi) \\ & - |r_{11}| |r_{12}| (\rho_{11} + \rho_{12}) \cos(\phi_{12} - \phi_{11} + \psi) \\ & + |r_{11}| |r_{12}| (\xi_{12} - \xi_{11}) \sin(\phi_{12} - \phi_{11} + \psi) \\ & + |r_{21}| |r_{22}| (\xi_{21} - \xi_{22}) \sin(\phi_{21} - \phi_{22} - \psi)], \quad (\text{B2}) \end{aligned}$$

$$\begin{aligned} \Delta_{ry} = & -\cot \theta_i [(f_p^2 + f_s^2) |r_{22}| |r_{21}| \sin(\phi_{21} - \phi_{22}) \\ & + 2 f_s^2 |r_{22}| |r_{12}| \sin(\phi_{22} - \phi_{12}) \\ & + f_p^2 |r_{21}| |r_{11}| \sin(\phi_{21} - \phi_{11}) \\ & + (f_p^2 + f_s^2) |r_{12}| |r_{11}| \sin(\phi_{11} - \phi_{12}) \\ & + 2 f_p f_s |r_{21}| |r_{12}| \sin(\phi_{21} - \phi_{12} - \psi) \\ & + 2 f_p f_s |r_{11}| |r_{22}| \sin(\phi_{22} - \phi_{11} + \psi) \\ & + f_p f_s (|r_{11}|^2 + |r_{12}|^2 + |r_{21}|^2 + |r_{22}|^2) \sin \psi], \quad (\text{B3}) \end{aligned}$$

$$\begin{aligned} \delta_{ry} = & -\cot \theta_i \{ (f_p^2 - f_s^2) [|r_{11}| |r_{12}| \cos(\phi_{12} - \phi_{11}) \\ & + |r_{21}| |r_{22}| \cos(\phi_{21} - \phi_{22})] \\ & + f_p f_s (|r_{22}|^2 - |r_{21}|^2 + |r_{12}|^2 - |r_{11}|^2) \cos \psi \}, \quad (\text{B4}) \end{aligned}$$

$$\begin{aligned} \tau = & f_s^2 (|r_{22}|^2 + |r_{12}|^2) + f_p^2 (|r_{11}|^2 + |r_{21}|^2) \\ & + 2 f_p f_s \{ |r_{22}| |r_{21}| \cos(\phi_{22} - \phi_{21} + \psi) \\ & + |r_{11}| |r_{12}| \cos(\phi_{12} - \phi_{11} + \psi) \}, \quad (\text{B5}) \end{aligned}$$

where $r_{aa'} = |r_{aa'}| \exp(i \phi_{aa'})$, $\rho_{aa'} = \text{Re}[\partial \ln r_{aa'} / \partial \theta_i]$, $\xi_{aa'} = \text{Im}[\partial \ln r_{aa'} / \partial \theta_i]$, and $a' = 1, 2$. For the RCP and LCP transmitted waves,

$$\begin{aligned} \Delta_{ax} = & n_a [f_p^2 (\xi_{11}^a |t_{11}^a|^2 + \xi_{21}^a |t_{21}^a|^2) + f_s^2 (\xi_{12}^a |t_{12}^a|^2 + \xi_{22}^a |t_{22}^a|^2)] \\ & + f_p^2 (\rho_{21}^a - \rho_{11}^a) |t_{11}^a| |t_{21}^a| \kappa \cos(\phi_{11}^a - \phi_{21}^a) + f_s^2 (\rho_{22}^a - \rho_{12}^a) |t_{12}^a| |t_{22}^a| \kappa \cos(\phi_{12}^a - \phi_{22}^a) \\ & + f_p^2 (\xi_{11}^a + \xi_{21}^a) |t_{11}^a| |t_{21}^a| \kappa \sin(\phi_{11}^a - \phi_{21}^a) + f_s^2 (\xi_{12}^a + \xi_{22}^a) |t_{12}^a| |t_{22}^a| \kappa \sin(\phi_{12}^a - \phi_{22}^a) \\ & + f_p f_s n_a |t_{11}^a| |t_{12}^a| \cos(\phi_{11}^a - \phi_{12}^a - \psi) (\xi_{11}^a + \xi_{12}^a) + f_p f_s \kappa |t_{11}^a| |t_{22}^a| \cos(\phi_{11}^a - \phi_{22}^a - \psi) (\rho_{22}^a - \rho_{11}^a) \\ & + f_p f_s n_a |t_{21}^a| |t_{22}^a| \cos(\phi_{21}^a - \phi_{22}^a - \psi) (\xi_{21}^a + \xi_{22}^a) + f_p f_s \kappa |t_{12}^a| |t_{21}^a| \cos(\phi_{12}^a - \phi_{21}^a - \psi) (\rho_{21}^a - \rho_{12}^a) \\ & + f_p f_s n_a |t_{11}^a| |t_{12}^a| \sin(\phi_{11}^a - \phi_{12}^a - \psi) (\rho_{11}^a - \rho_{12}^a) + f_p f_s n_a |t_{11}^a| |t_{22}^a| \sin(\phi_{11}^a - \phi_{22}^a - \psi) (\xi_{11}^a + \xi_{22}^a) \\ & + f_p f_s n_a |t_{21}^a| |t_{22}^a| \sin(\phi_{21}^a - \phi_{22}^a - \psi) (\rho_{21}^a - \rho_{22}^a) + f_p f_s n_a |t_{12}^a| |t_{21}^a| \sin(\phi_{12}^a - \phi_{21}^a - \psi) (\xi_{12}^a + \xi_{21}^a), \quad (\text{B6}) \end{aligned}$$

$$\begin{aligned} \delta_{ax} = & n_a [f_p^2 (\rho_{11}^a |t_{11}^a|^2 + \rho_{21}^a |t_{21}^a|^2) + f_s^2 (\rho_{12}^a |t_{12}^a|^2 + \rho_{22}^a |t_{22}^a|^2)] + f_p^2 (\xi_{11}^a - \xi_{21}^a) |t_{11}^a| |t_{21}^a| \kappa \cos(\phi_{11}^a - \phi_{21}^a) \\ & + f_s^2 (\xi_{12}^a - \xi_{22}^a) |t_{12}^a| |t_{22}^a| \kappa \cos(\phi_{12}^a - \phi_{22}^a) + f_p^2 (\rho_{11}^a + \rho_{21}^a) |t_{11}^a| |t_{21}^a| \kappa \sin(\phi_{11}^a - \phi_{21}^a) \\ & + f_s^2 (\rho_{12}^a + \rho_{22}^a) |t_{12}^a| |t_{22}^a| \kappa \sin(\phi_{12}^a - \phi_{22}^a) + f_p f_s n_a |t_{11}^a| |t_{12}^a| \cos(\phi_{11}^a - \phi_{12}^a - \psi) (\rho_{11}^a + \rho_{12}^a) \\ & + f_p f_s \kappa |t_{11}^a| |t_{22}^a| \cos(\phi_{11}^a - \phi_{22}^a - \psi) (\xi_{11}^a - \xi_{22}^a) + f_p f_s n_a |t_{21}^a| |t_{22}^a| \cos(\phi_{21}^a - \phi_{22}^a - \psi) (\rho_{21}^a + \rho_{22}^a) \\ & + f_p f_s \kappa |t_{12}^a| |t_{21}^a| \cos(\phi_{12}^a - \phi_{21}^a - \psi) (\xi_{12}^a - \xi_{21}^a) + f_p f_s n_a |t_{11}^a| |t_{12}^a| \sin(\phi_{11}^a - \phi_{12}^a - \psi) (\xi_{12}^a - \xi_{11}^a) \end{aligned}$$

$$\begin{aligned}
& + f_p f_s n_a |t_{11}^a| |t_{22}^a| \sin(\phi_{11}^a - \phi_{22}^a - \psi)(\rho_{11}^a + \rho_{22}^a) + f_p f_s n_a |t_{21}^a| |t_{22}^a| \sin(\phi_{21}^a - \phi_{22}^a - \psi)(\xi_{22}^a - \xi_{21}^a) \\
& + f_p f_s n_a |t_{12}^a| |t_{21}^a| \sin(\phi_{12}^a - \phi_{21}^a - \psi)(\rho_{12}^a + \rho_{21}^a), \tag{B7} \\
\Delta_{ay} = & -\cot\theta_i \left[-f_p^2 (|t_{11}^a|^2 + |t_{21}^a|^2) - f_s^2 (|t_{12}^a|^2 + |t_{22}^a|^2) \right] \eta_a \kappa + \kappa (f_p^2 + f_s^2) [|t_{11}^a| |t_{22}^a| \cos(\phi_{11}^a - \phi_{22}^a) \\
& - |t_{12}^a| |t_{21}^a| \cos(\phi_{12}^a - \phi_{21}^a)] - 2f_p f_s \eta_a \cos\psi \left[\kappa |t_{11}^a| |t_{12}^a| \cos(\phi_{11}^a - \phi_{12}^a) + \kappa |t_{21}^a| |t_{22}^a| \cos(\phi_{21}^a - \phi_{22}^a) \right. \\
& + n_a |t_{12}^a| |t_{21}^a| \sin(\phi_{12}^a - \phi_{21}^a) + n_a |t_{11}^a| |t_{22}^a| \sin(\phi_{11}^a - \phi_{22}^a) \left. \right] - n_a \{ (f_p^2 + f_s^2) |t_{11}^a| |t_{12}^a| \sin(\phi_{11}^a - \phi_{12}^a) \\
& + 2\eta_a [f_p^2 |t_{11}^a| |t_{21}^a| \sin(\phi_{11}^a - \phi_{21}^a) + f_s^2 |t_{12}^a| |t_{22}^a| \sin(\phi_{12}^a - \phi_{22}^a)] \} - (f_p^2 + f_s^2) n_a |t_{21}^a| |t_{22}^a| \sin(\phi_{21}^a - \phi_{22}^a)_s \\
& - f_p f \{ n_a (|t_{11}^a|^2 + |t_{12}^a|^2 + |t_{21}^a|^2 + |t_{22}^a|^2) + 2n_a \eta_a [|t_{12}^a| |t_{21}^a| \cos(\phi_{12}^a - \phi_{21}^a) - |t_{11}^a| |t_{22}^a| \cos(\phi_{11}^a - \phi_{22}^a)] \} \\
& + 2\kappa [|t_{11}^a| |t_{12}^a| \eta_a \sin(\phi_{11}^a - \phi_{12}^a) + |t_{11}^a| |t_{21}^a| \sin(\phi_{11}^a - \phi_{21}^a) + |t_{12}^a| |t_{22}^a| \sin(\phi_{12}^a - \phi_{22}^a) + |t_{21}^a| |t_{22}^a| \sin(\phi_{21}^a - \phi_{22}^a)] \sin(\psi), \tag{B8}
\end{aligned}$$

$$\begin{aligned}
\delta_{ay} = & \cot\theta_i \left\{ (f_s^2 - f_p^2) \left[n_a [|t_{11}^a| |t_{12}^a| \cos(\phi_{11}^a - \phi_{12}^a) + |t_{21}^a| |t_{22}^a| \cos(\phi_{21}^a - \phi_{22}^a)] + \kappa [|t_{11}^a| |t_{22}^a| \sin(\phi_{11}^a - \phi_{22}^a) \right. \right. \\
& \left. \left. + |t_{12}^a| |t_{21}^a| \sin(\phi_{12}^a - \phi_{21}^a)] \right\} + f_p f_s \cos\psi \{ n_a (|t_{11}^a|^2 - |t_{12}^a|^2 + |t_{21}^a|^2 - |t_{22}^a|^2) \right. \\
& \left. + 2\kappa [|t_{11}^a| |t_{21}^a| \sin(\phi_{11}^a - \phi_{21}^a) - |t_{12}^a| |t_{22}^a| \sin(\phi_{12}^a - \phi_{22}^a)] \right\}, \tag{B9}
\end{aligned}$$

$$\begin{aligned}
\tau_a = & n_a [f_p^2 (|t_{11}^a|^2 + |t_{21}^a|^2) + f_s^2 (|t_{12}^a|^2 + |t_{22}^a|^2)] + 2f_p f_s n_a [|t_{11}^a| |t_{12}^a| \cos(\phi_{11}^a - \phi_{12}^a - \psi) \\
& + |t_{21}^a| |t_{22}^a| \cos(\phi_{21}^a - \phi_{22}^a - \psi)] + 2\kappa [f_s^2 |t_{12}^a| |t_{22}^a| \sin(\phi_{12}^a - \phi_{22}^a) + f_p^2 |t_{11}^a| |t_{21}^a| \sin(\phi_{11}^a - \phi_{21}^a) \\
& + f_p f_s |t_{11}^a| |t_{22}^a| \sin(\phi_{11}^a - \phi_{22}^a - \psi) + f_p f_s |t_{12}^a| |t_{21}^a| \sin(\phi_{12}^a - \phi_{21}^a + \psi)], \\
[1pt] t_{aa'}^a = & |t_{aa'}^a| \exp(i\phi_{aa'}^a), \quad \rho_{aa'}^a = \text{Re}[\partial \ln t_{aa'}^a / \partial \theta_i], \quad \xi_{aa'}^a = \text{Im}[\partial \ln t_{aa'}^a / \partial \theta_i]. \tag{B10}
\end{aligned}$$

-
- [1] J. Sinova, D. Culcer, Q. Niu, N. A. Sinitsyn, T. Jungwirth, and A. H. MacDonald, *Phys. Rev. Lett.* **92**, 126603 (2004).
- [2] S. Murakami, N. Nagaosa, and S. C. Zhang, *Science* **301**, 1348 (2003).
- [3] J. Wunderlich, B. Kaestner, J. Sinova, and T. Jungwirth, *Phys. Rev. Lett.* **94**, 047204 (2005).
- [4] M. Onoda, S. Murakami, and N. Nagaosa, *Phys. Rev. Lett.* **93**, 083901 (2004); *Phys. Rev. E* **74**, 066610 (2006).
- [5] K. Y. Bliokh and Y. P. Bliokh, *Phys. Rev. Lett.* **96**, 073903 (2006); *Phys. Rev. E* **75**, 066609 (2007).
- [6] Chun-Fang Li, *Phys. Rev. A* **76**, 013811 (2007).
- [7] A. Aiello and J. P. Woerdman, *Opt. Lett.* **33**, 1437 (2008).
- [8] V. G. Fedoseyev, *Opt. Commun.* **282**, 1247 (2009).
- [9] O. Hosten and P. Kwiat, *Science* **319**, 787 (2008).
- [10] Y. Qin, Y. Li, H. Y. He, and Q. H. Gong, *Opt. Lett.* **34**, 2551 (2009); *Opt. Express* **18**, 16832 (2010).
- [11] A. Kavokin, G. Malpuech, and M. Glazov, *Phys. Rev. Lett.* **95**, 136601 (2005).
- [12] C. Leyder, M. Romanelli, J. P. Karr, E. Giacobino, T. C. H. Liew, M. M. Glazov, A. V. Kavokin, G. Malpuech, and A. Bramati, *Nature Phys.* **3**, 628 (2007).
- [13] K. Y. Bliokh, Y. Gorodetski, V. Kleiner, and E. Hasman, *Phys. Rev. Lett.* **101**, 030404 (2008).
- [14] K. Y. Bliokh, A. Niv, V. Kleiner, and E. Hasman, *Nature Photon.* **2**, 748 (2008).
- [15] D. Haefner, S. Sukhov, and A. Dogariu, *Phys. Rev. Lett.* **102**, 123903 (2009).
- [16] A. Aiello, N. Lindlein, C. Marquardt, and G. Leuchs, *Phys. Rev. Lett.* **103**, 100401 (2009).
- [17] M. Merano, A. Aiello, M. P. van Exter, and J. P. Woerdman, *Nature Photonics* **3**, 337 (2009).
- [18] J.-M. Ménard, A. E. Mattacchione, H. M. van Driel, C. Hautmann, and M. Betz, *Phys. Rev. B* **82**, 045303 (2010).
- [19] D. R. Smith, W. J. Padilla, D. C. Vier, S. C. Nemat-Nasser, and S. Schultz, *Phys. Rev. Lett.* **84**, 4184 (2000); R. A. Shelby, D. R. Smith, and S. Schultz, *Science* **292**, 77 (2001).
- [20] J. B. Pendry, *Phys. Rev. Lett.* **85**, 3966 (2000).
- [21] V. M. Agranovich and Y. N. Gartstein, *Phys. Usp.* **49**, 1029 (2006).
- [22] C. M. Soukoulis, S. Linden, and M. Wegener, *Science* **315**, 47 (2007).
- [23] V. G. Veselago, *Sov. Phys. Usp.* **10**, 509 (1968).
- [24] H. Luo, S. Wen, W. Shu, Z. Tang, Y. Zou, and D. Fan, *Phys. Rev. A* **80**, 043810 (2009).
- [25] C. M. Krowne, *Phys. Lett. A* **373**, 466 (2009).
- [26] S. Tretyakov, I. Nefedov, A. Sihvola, S. Maslovski, and C. Simovski, *J. Electromagn. Waves Appl.* **17**, 695 (2003).
- [27] J. B. Pendry, *Science* **306**, 1353 (2004).
- [28] J. Zhou, J. Dong, B. Wang, T. Koschny, M. Kafesaki, and C. M. Soukoulis, *Phys. Rev. B* **79**, 121104 (2009).
- [29] B. Wang, J. Zhou, T. Koschny, and C. M. Soukoulis, *Appl. Phys. Lett.* **94**, 151112 (2009).
- [30] S. Zhang, Y.-S. Park, J. Li, X. Lu, W. Zhang, and X. Zhang, *Phys. Rev. Lett.* **102**, 023901 (2009).

- [31] B. Wang, J. Zhou, T. Koschny, M. Kafesaki, and C. M. Soukoulis, *J. Opt. A: Pure Appl. Opt.* **11**, 114003 (2009).
- [32] A. V. Rogacheva, V. A. Fedotov, A. S. Schwanecke, and N. I. Zheludev, *Phys. Rev. Lett.* **97**, 177401 (2006).
- [33] J. K. Gansel, M. Thiel, M. S. Rill, M. Decker, K. Bade, V. Saile, G. von Freymann, S. Linden, and M. Wegener, *Science* **325**, 1513 (2009).
- [34] W. T. Dong, L. Gao, and C. W. Qiu, *Prog. Electromagn. Res.* **104**, 255 (2009).